The RhoA/ROCK-I/MLC pathway is involved in the ethanol-induced apoptosis by anoikis in astrocytes

Rebeca Miñambres, Rosa M. Guasch, Amparo Perez-Aragó and Consuelo Guerri*

Department of Cellular Pathology, Centro de Investigación Príncipe Felipe, c/EP Autopista del Saler 16-3, 46013-Valencia, Spain
*Author for correspondence (e-mail: guerri@ochoa.fib.es)

Accepted 3 October 2005
Journal of Cell Science 119, 271-282 Published by The Company of Biologists 2006
doi:10.1242/jcs.02723

Summary

Anoikis is a programmed cell death induced by loss of anchorage that is involved in tissue homeostasis and disease. Ethanol is an important teratogen that induces marked central nervous system (CNS) dysfunctions. Here we show that astrocytes exposed to ethanol undergo morphological changes associated with anoikis, including the peripheral reorganization of both focal adhesions and actin-myosin system, cell contraction, membrane blebbing and chromatin condensation. We found that either the small GTPase RhoA or its effector ROCK-I (Rho kinase), promotes membrane blebbing in astrocytes. Ethanol induces a ROCK-I activation that is mediated by RhoA, rather than by caspase-3 cleavage. Accordingly, the RhoA inhibitor C3, completely abolishes the ethanol-induced ROCK-I activation. Furthermore, inhibition of both RhoA and ROCK prevents the membrane blebbing induced by ethanol. Ethanol also promotes myosin light chain (MLC) phosphorylation, which might be involved in the actin-myosin contraction. All of these findings strongly support that ethanol-exposed astrocytes undergo apoptosis by anoikis and also that the RhoA/ROCK-I/MLC pathway participates in this process.

Key words: Anoikis, Blebbing, RhoA, ROCK-I, Ethanol, Astrocytes

Introduction

Cell anchorage not only provides a structural support but also mediates crucial survival signals. Disturbances of cell attachments frequently lead to the initiation of a suicide program named anoikis. Considering that cell anchorage is a remarkably complex process involving several adhesion molecules, cytoskeletal elements and signalling pathways it is unlikely that a single mechanism will exist in the anoikis process (Grossmann, 2002). Therefore, anoikis is a very useful tool to study the complex balance between life and death that determines the fate of a cell, being able to identify pathways that are relevant for survival or death, under physiological and pathological conditions (Grossmann, 2002).

The apoptosis process is characterized by morphological changes in the cell, which include cell contraction, dynamic membrane blebbing and chromosome condensation. During the execution phase of this process, cells undergo a series of events, such as rearrangement of actin-myosin into a peripheral ring, release of the extracellular matrix attachments (ECM), reorganization of focal adhesions and adoption of a rounded morphology (Mills et al., 1999). The force required to produce membrane blebbing is generated by the actin-myosin system (Torgerson and McNiven, 1998). Several studies revealed just how important the Rho signalling pathway actually is in regulating the morphological changes observed during apoptosis (Coleman and Olson, 2002).

Rho GTPases control many cellular activities other than the cytoskeleton and cell adhesion, such as cell polarity, endocytosis, vesicle trafficking, cell proliferation, differentiation, oncogenesis and gene transcription (Burridge and Wennerberg, 2004). Based on primary sequence and known functions, the 20 Rho proteins can be divided into five groups: the Rho-like, Rac-like, Cdc42-like, Rnd and RhoBTB subfamilies (Burridge and Wennerberg, 2004). It has been recently proposed that Rho induces myosin contractility and that the resulting tension drives the formation of stress fibres and focal adhesions (Chrzanowska-Wodnicka and Burridge, 1996). In fact, RhoA has been implicated in the contraction observed in apoptotic cells (Mills et al., 1998).

ROCKs were the first effectors of Rho to be discovered and they were initially characterized for their roles in mediating the formation of RhoA-induced stress fibres and focal adhesions (Ishizaki et al., 1996; Leung et al., 1996). ROCK is a serine/threonine kinase that can directly phosphorylate the myosin light chain (MLC) or indirectly increase MLC phosphorylation (MLC-pp) by inactivating the myosin phosphatase (Amano et al., 1996; Kimura et al., 1996). There are two ROCK isoforms: ROCK-I (also known as ROKβ and p160ROCK) and ROCK-II (also known as ROKα and Rho kinase), which share 65% amino acid homology, and the proteins show the highest similarity in their kinase domains (92% identity). Activated Rho binds to ROCKs and disrupts the negative regulatory interaction between the kinase domain and the autoinhibitory region, resulting in an open conformation that frees the catalytic activity (Coleman et al., 2001; Sebbagh et al., 2001). In addition, it has been shown that only ROCK-I can be cleaved by caspase-3 during apoptosis, generating an active form of the kinase that induces membrane blebbing (Coleman et al., 2001; Sebbagh et al., 2001).

Glial cells and their interactions with neurons play crucial roles in the mammalian central nervous system development (Fields and Stevens-Graham, 2002). Indeed, astroglial cells control the rearrangement and elimination of the synaptic junctions, as well as the formation of functional synapses

(Mauch et al., 2001; Ullian et al., 2001) and they are involved in the exchange of nutrients, neurotransmitters, ions and growth factors (Fields and Stevens-Graham, 2002; Nedergaard et al., 2003; Newman, 2003). In addition, disturbances in glial cells or in neuronal-glial interactions during crucial periods of brain development may induce irreversible deficits in the CNS function (Crespel et al., 2002; Laure-Kamionowska et al., 2002), that demonstrate the potential role that glia play in brain development and integrity. Interestingly, it has been recently demonstrated that glial cells are a multipotent neural stem cell (Anthony et al., 2004; Doetsch, 2003; Sanai et al., 2004).

Much evidence exists regarding the developing brain sensitivity to damage from environmental toxic compounds (Costa et al., 2004), and experimental evidence also suggests that glial cells are susceptible to neurotoxic agents (Aschner et al., 1999). Ethanol is one of the most important teratogens that profoundly affect the developing foetal brain, and its consumption during gestation can produce mental retardation and neurobehavioural disorders, as well as foetal alcohol syndrome (FAS) (Guerri, 2002). Astroglial cells are affected by prenatal ethanol exposure (Valles et al., 1997), which suggests that alterations in glial-neuron interactions may underlie the CNS abnormalities associated with ethanol-induced neurotoxic effects (Eriksen and Druse, 2001; Guerri and Renau-Piqueras, 1997; Valles et al., 1997). Indeed, we have reported that in vivo alcohol exposure induces astroglial death (Climent et al., 2002), and we recently demonstrated that ethanol induces a reorganization of both the actin cytoskeleton and focal adhesions in astrocytes (Guasch et al., 2003). Interestingly, these changes mimic some of the features observed during the initial steps of an anoikis process (Mills et al., 1999). Since the small Rho GTPases have been implicated in apoptosis (Coleman and Olson, 2002), we asked whether ethanol induces an apoptosis by anoikis in astrocytes and whether the RhoA signalling pathway participates in the morphological changes associated with anoikis. Here we report that astrocytes undergo apoptosis by anoikis when exposed to ethanol and that this process is mediated by the RhoA/ROCK-I/MLC pathway. Our findings also suggest that caspase-3-mediated ROCK-I activation is not involved in this process.

Results

Astrocytes die by apoptosis when exposed to ethanol

To investigate whether acute ethanol treatment induces apoptosis in cultured cortical astrocytes, different concentrations of alcohol (100 and 200 mM) were added to the growth culture medium and DNA fragmentation was studied after different times of ethanol exposure (3, 6, 14 and 24 hours). Astrocytes were incubated with propidium iodide (PI) to stain the DNA and analysis by fluorescence-activated cell sorting (FACS) was performed. This procedure has been shown to be the best quantitative technique to detect apoptosis in astrocytes (Micoud et al., 2001). Ethanol significantly increased the proportion of astrocytes in the sub-G0/G1 population, in all the time-points analyzed (Fig. 1A). Interestingly, the elevation in this apoptotic population was detected as early as 3 hours upon ethanol addition (in each alcohol concentration tested). Furthermore, pre-treatment of astrocytes with the pan-caspase inhibitor z-VAD-fmk abolished the ethanol-induced increase in the sub-G0/G1 population (Fig. 1B), suggesting that ethanol promotes caspase-dependent apoptosis in astrocytes. These findings are in accordance with recent studies where DNA fragmentation was detected in astrocytes exposed to ethanol for 24 hours (Pascual et al., 2003).

To analyze further the apoptosis induced by ethanol, the caspase-3 activity in astrocytes exposed to ethanol was also assessed. The same experimental conditions were used for these experiments, including alcohol concentrations as well as the ethanol exposure time, as those performed to detect the sub-G0/G1 population. The caspase-3 activity significantly rose as early as 3 hours of ethanol exposure, as shown in Fig. 1C, and then the activity progressively increased until a peak at 14 hours upon ethanol treatment is reached. Accordingly, pretreatment of astrocytes with a caspase-3 inhibitor, z-VAD-fmk, abolished the ethanol-induced activation of caspase-3 (Fig. 1D).

We further analyzed apoptosis by labelling astrocytes exposed to ethanol with annexin V-PE, a marker of the early stage of apoptosis which reveals the lost of plasma membrane asymmetry (Herault et al., 1999). To distinguish necrotic cells from apoptotic cells, the annexin V analysis was performed simultaneously with a dye-exclusion stain, 7-amino-actinomycin D (7-AAD) (Herault et al., 1999; Vermes et al., 1995). Indeed, flow cytometric analysis showed a maximum increase in the early apoptotic population (7-AAD$^-$ annexinV-PE$^+$) at 3 hours of ethanol exposure, decreasing thereafter (Fig. 1E). Taken together, these results indicate that ethanol is able to induce apoptosis in astrocytes and we demonstrated for the first time that this apoptosis occurs as early as 3 hours of ethanol treatment.

Morphological changes associated with the ethanol-induced apoptosis in astrocytes

Apoptosis is a dynamic process characterized by the activation of caspases that are responsible for some morphological changes, including membrane blebbing and cell contraction (Coleman and Olson, 2002). One of the first morphological changes observed during apoptosis is the partial detachment from the extracellular matrix, adopting the cell a rounded morphology (Mills et al., 1999). This process is most dramatic in cells that are spread out with firm attachments and stress fibres, such as cultured cortical astrocytes (Figs 2Aa,b). Therefore, to investigate whether these morphological changes also occurred in astrocytes exposed to alcohol, cells were exposed to 100 mM ethanol for 3 hours and the actin, myosin and chromatin condensation were studied by immunofluorescence.

Fig. 2Ad illustrates that astrocytes exposed to ethanol loose stress fibres, adopt a more rounded morphology and reorganize the actin into a peripheral membrane-associated ring. Interestingly, similar alterations in actin reorganization have been previously observed in astrocytes exposed chronically to ethanol (Guasch et al., 2003).

Previous studies have suggested that during the apoptosis, myosin-dependent contraction of the actin ring is followed by a period of dynamic plasma membrane protrusion and retraction, leading to the blebbing stage (Mills et al., 1999). Therefore, we asked whether the ethanol-induced actin ring colocalizes with myosin and whether this actin-myosin ring could lead to membrane blebbing and chromatin condensation. Fig. 2Ae illustrates that ethanol-treated astrocytes showed a

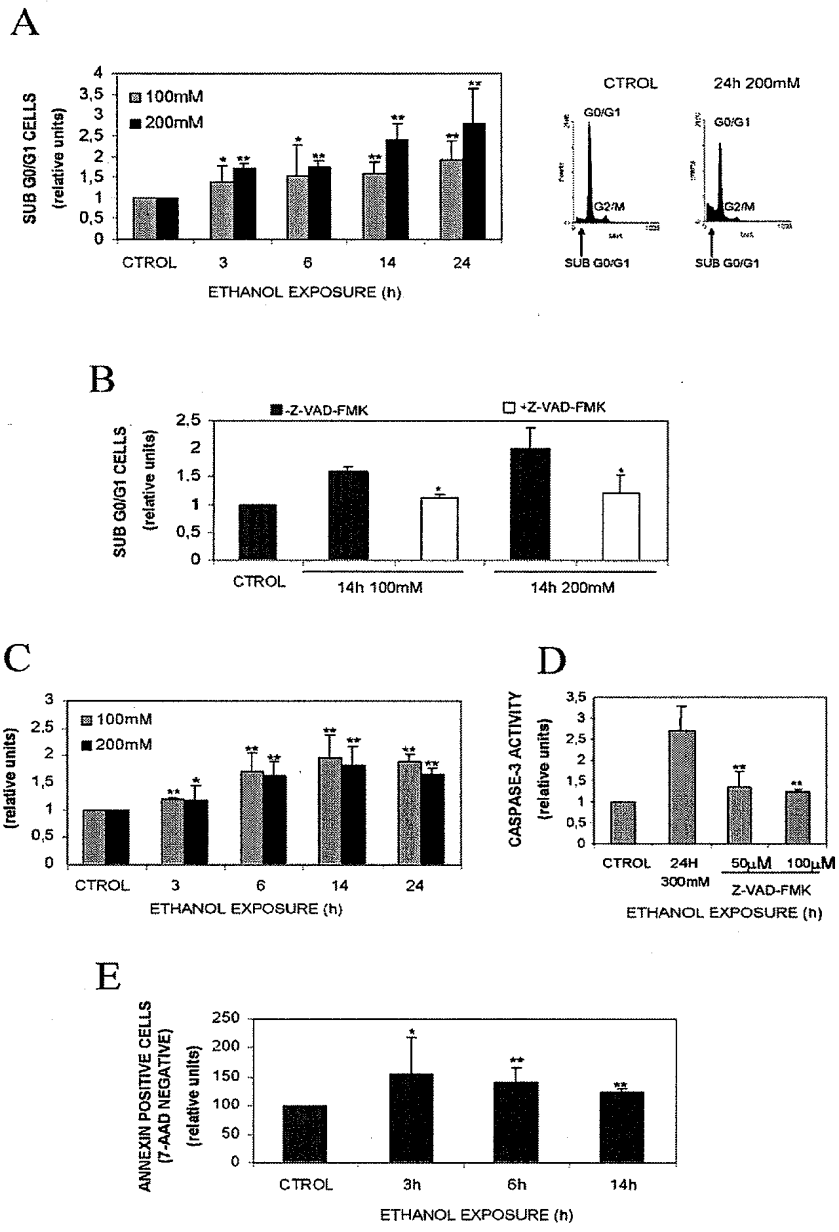

Fig. 1. Ethanol exposure induces apoptosis in astrocytes. Astrocytes were exposed to 100 and 200 mM ethanol concentrations for 3, 6, 14 and 24 hours. (A) The sub-G0/G1 astrocyte population, quantified by flow cytometry, increases after ethanol exposure. Representative histograms are shown for control and 200 mM ethanol-treated samples (for 24 hours). (B) Inhibition of the sub-G0/G1 population with the pan-caspase inhibitor z-VAD-fmk (100 μM), at two different ethanol concentrations (100 and 200 mM). (C) Ethanol increases the caspase-3 activity. (D) Preincubation with z-VAD-fmk (50 and 100 μM) abolishes ethanol-induced caspase-3 activation (300 mM for 24 hours). (E) Quantification of early apoptosis using annexin-V together with 7-AAD and detected by flow cytometry. Values are mean ±s.d. of five different experiments. $*P<0.05$ and $**P<0.001$ versus control values in one-way ANOVA.

colocalization of actin-myosin in a peripheral ring, along with cell contraction and membrane blebbing (Figs 2Ag,h). Concomitantly, most of ethanol-treated astrocytes displayed chromatin condensation (Fig. 2Ai) as well as nuclear fragmentation (Fig. 2Al), a characteristic event during late apoptosis (Figs 2Aj,k).

A statistical analysis of the aforementioned morphological changes in astrocytes demonstrated that ethanol significantly increased peripheral actin reorganization, blebbing and chromatin condensation (Fig. 2B). It is interesting to note that the morphological changes induced by ethanol were observed as early as one hour after ethanol exposure, which is in accordance with the apoptotic process duration (Mills et al., 1999). We further observed that ethanol-induced actin reorganization and blebbing reached a maximum value at 6 hours after 100 mM ethanol exposure and that a slight decrease was noted after 14 hours. Notably, we observed that the levels of caspase-3 activity are maximal after a 14 hours ethanol exposure (100 mM), which suggests that the abovementioned morphological changes represent sequential stages within the execution phase of apoptosis (Mills et al., 1999).

Astrocytes exposed to ethanol undergo apoptosis by anoikis

To investigate further whether the ethanol-induced apoptosis in astrocytes is an anoikis process that starts with a partial detachment from the extracellular matrix (Mills et al., 1999), we next studied the effect of ethanol on focal adhesion complexes. For this purpose, astrocytes were exposed to ethanol (100 mM) for 1 hour, and then the paxillin (focal adhesion protein) was assessed by immunofluorescence.

It is known that during the anoikis process, focal adhesion complexes disassemble and reconcentrate ventrally underneath the newly rounded cell (Huot et al., 1998; Mills et al., 1999). Fig. 3Aa showed that control astrocytes displayed stress fibres attached to the substratum by focal adhesion proteins as paxillin, that is visualized as a dot-like staining (Fig. 3Ab). However, when cells were exposed to ethanol we observed a reorganization of focal adhesion complexes (Fig. 3Ad) at the

periphery of the actin rings (Fig. 3Ac), together with a decrease in their content. Indeed, the paxillin staining mostly disappears when cells are densely packed (Figs 3Ae,f). However, by western blot analysis we observed that the earliest reduction in the paxillin levels is about 3 hours of ethanol exposure, suggesting that the immunofluorescence technique is more sensitive to detect this type of changes (Fig. 3B). Furthermore, by western blot analysis we confirmed that ethanol significantly decreased the levels of paxillin in a dose-dependent manner (Fig. 3C).

It has been demonstrated that apoptosis is preceded by an early tyrosine dephosphorylation of some focal adhesion proteins such as FAK (van de Water et al., 1999) and paxillin (Bannerman et al., 1998), events closely associated with loss of the cell-matrix interactions that are sufficient to initiate anoikis (van de Water et al., 1999). To assess further whether these events also occur in astrocytes exposed to ethanol, phosphotyrosine staining was analyzed in cells treated to ethanol (100 mM) for 1 hour. Immunofluorescence analysis indicated that phosphotyrosine is located at the end of stress fibres (Fig. 3Ca) in control astrocytes, showing a punctuate pattern (Fig. 3Cb). However, cells treated with 100 mM ethanol displayed a peripheral reorganization (Fig. 3Cc) together with a significant reduction in phosphotyrosine immunostaining (Fig. 3Cd), which is scarcely detected (Fig. 3Cf) when cells are densely packed (Fig. 3Ce), as in the case of paxillin. It is worth noting that these alterations in focal adhesion proteins are already observed at 15 minutes of ethanol treatment. Taken together, these results suggest that astrocytes exposed to ethanol undergo a sequence of morphological changes associated with a form of cell death termed anoikis.

V14RhoA and active ROCK-I induce membrane blebbing and chromatin condensation in cortical astrocytes

It has been proposed that the actin-myosin system is the driving power that promotes cell contraction and the formation of membrane blebs and apoptotic bodies (Coleman and Olson, 2002). Recent studies have also demonstrated the Rho signalling pathway involvement in regulating the morphological changes observed in the apoptotic process (Coleman and Olson, 2002). Therefore, we next explored whether RhoA and ROCK-I, an effector of RhoA, could induce membrane blebbing and chromatin condensation in astrocytes.

For this purpose, astrocytes were cotransfected with an expression vector containing either active RhoA (V14RhoA) or an inactive mutant of RhoA

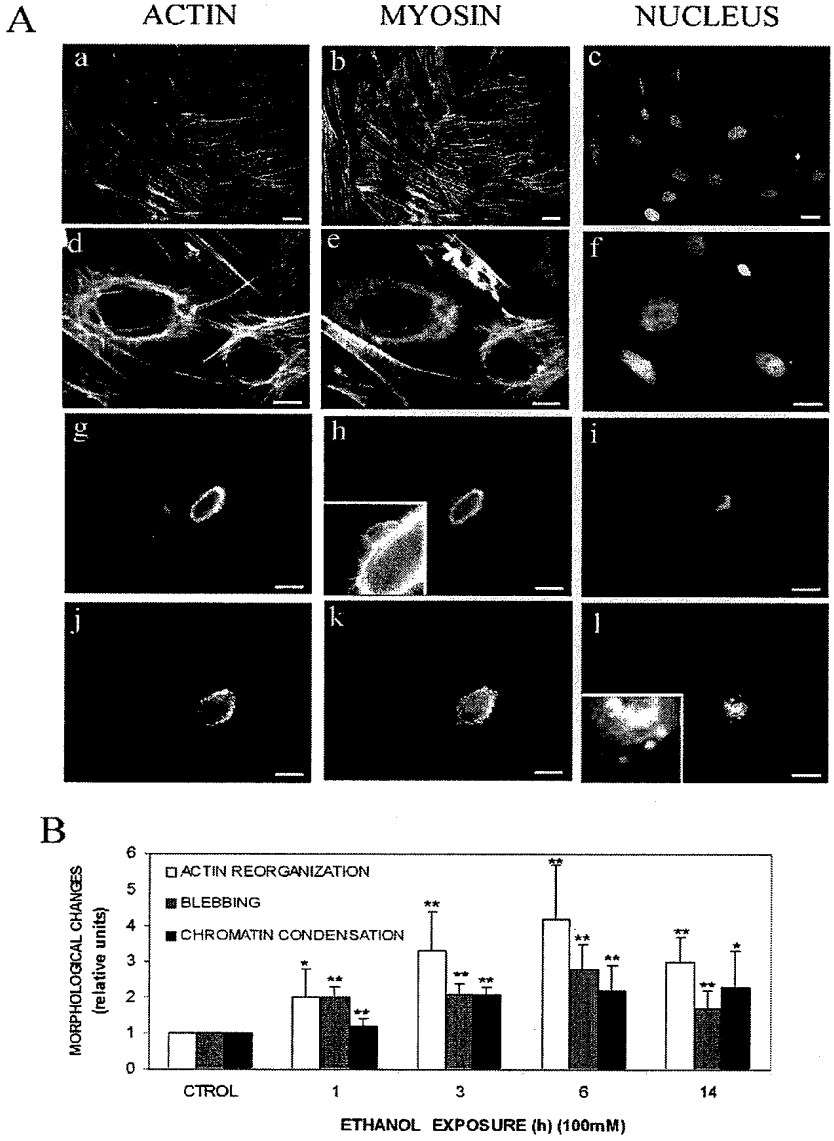

Fig. 2. Astrocytes exposed to ethanol show morphological changes associated with apoptosis. (A) Cells were incubated with 100 mM ethanol for 1 hour. Actin (a,d,g,j), myosin (b,e,h,k) and nuclei (c,f,i,l) were analyzed by immunofluorescence. Cultured astrocytes show F-actin (a) and myosin (b) colocalization, running throughout the cytoplasm. Ethanol induces an actin-myosin reorganization into a peripheral ring (d,e) that leads to membrane blebbing (g,h,j,k) and chromatin condensation (i), as well as nuclear fragmentation (l). (B) Quantification of morphological apoptotic features such as actin reorganization, membrane blebbing and chromatin condensation at 1, 3, 6 and 14 hours in alcohol-exposed cells (100 mM). The values shown are means ±s.d. from four different primary cultures and more than 300 cells were counted for each experiment. Asterisks indicate significant differences when referred to control samples (*P<0.01 and **P<0.001 by a one-way ANOVA test). Bars, 10 μm.

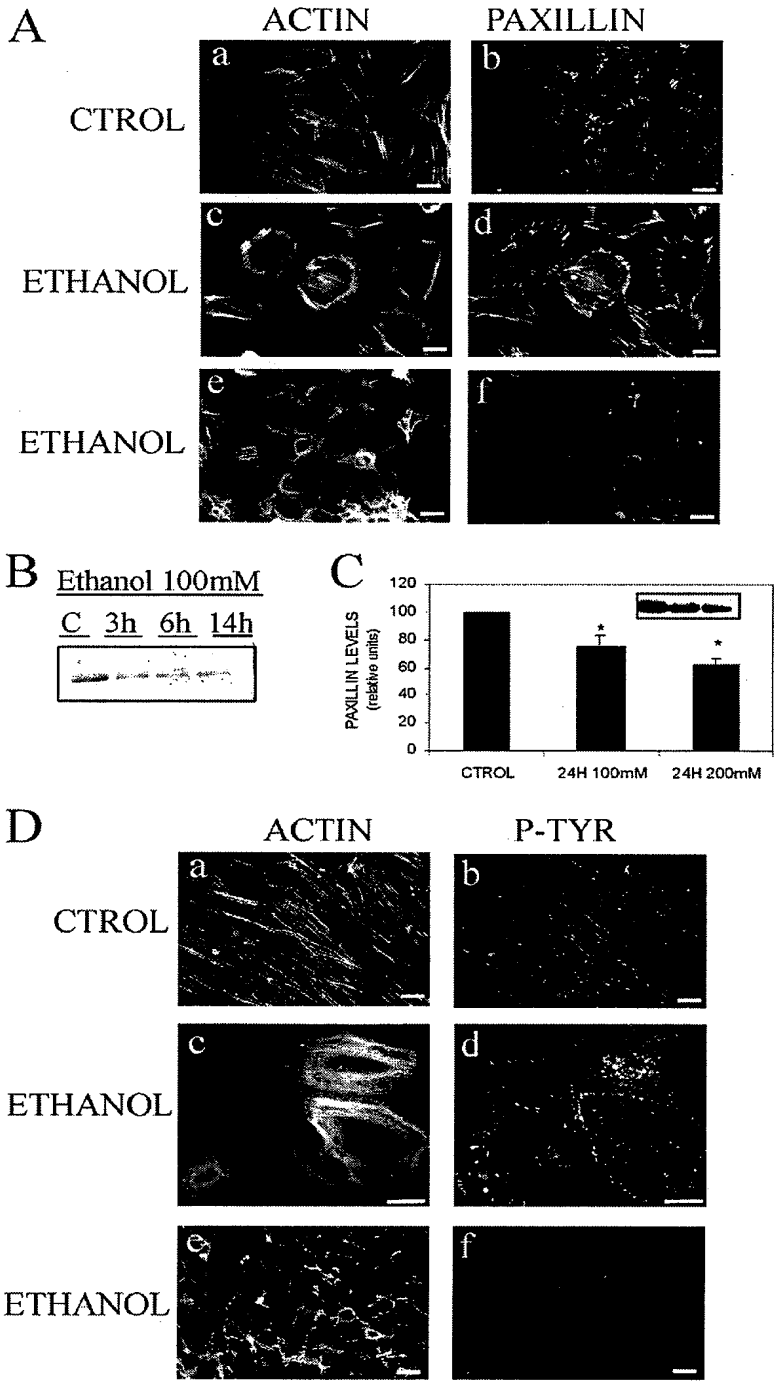

Fig. 3. Ethanol reorganizes focal adhesions and decreases their levels. Astrocytes were exposed to 100 mM ethanol for an hour. (A) Actin (a,c,e) and paxillin (b,d,f) were detected by immunofluorescence. Control astrocytes show a punctuate pattern of paxillin (b). Ethanol treatment causes a paxillin reorganization at the cell periphery (d) and dramatically decreases its content when cells are densely packed (f). (B) A representative western blot of paxillin from control- and ethanol-treated cells, at different times of alcohol exposure. (C) Densitometric quantification of paxillin staining at two ethanol concentrations (100 and 200 mM for 24 hours). Equal amount of protein was used (50 μg/well). The values represent means ±s.d. from four different cultures and they are expressed as percentages of the control value. Asterisks indicate significant differences with control sample (**P<0.001). (D) Astrocytes were double-stained for F-actin (a,c,e) and phosphotyrosine (b,d,f). Ethanol-exposed cells show a cortical reorganization (d) and a reduction in phosphotyrosine staining of the focal adhesion proteins (f). Bars, 10 μm.

(V14A37RhoA), which has low GTPase activity and is unresponsive to GTPase activating proteins (GAPs), together with a plasmid expressing the green fluorescent protein (GFP). Transfected cells were visualized in green and actin was detected by phalloidin staining (red). RhoA induced the formation of actin stress fibres together with membrane blebbing and chromatin condensation, as analyzed by Hoechst staining (Fig. 4A). None of these changes were observed in astrocytes expressing the inactive RhoA.

To assess further the effect of RhoA on the state of nuclear structure, a TUNEL staining was used to reveal the presence of DNA fragmentation. Astrocytes were transfected with a myc-tagged expression vector of V14RhoA and visualized in red (anti-myc), blue (Hoechst) and green (TUNEL). RhoA transfected cells showed chromatin condensation, as well as DNA fragmentation (Fig. 4B). In addition, statistical analysis showed that RhoA induced a significant increase in membrane blebbing, as well as in chromatin condensation (Fig. 4C).

To analyze the effects of ROCK-I, astrocytes were cotransfected with an expression vector encoding a constitutively active C-terminally truncated ROCK-I, ROCK-I-Δ1 (Ishizaki et al., 1997), together with a plasmid expressing the GFP. Immunofluorescence analysis revealed that astrocytes expressing active ROCK-I contained thick parallel or 'stellate' actin stress fibres (Fig. 4D), as has been previously demonstrated for different cell types (Amano et al., 1997; Coleman et al., 2001; Nakano et al., 1999). These actin changes were accompanied by cell contraction, membrane blebbing and chromatin condensation. Control experiments were performed using a ROCK-I-truncated mutant, ROCK-I-Δ5, that closely corresponds to the kinase domain and has no effect on the actin organization of astrocytes, as previously reported for HeLa cells (Ishizaki et al., 1997). Astrocytes expressing ROCK-I-Δ5 showed neither blebs nor condensation of the nucleus.

We also studied the effect of ROCK-I on the state of nuclear chromatin by using the TUNEL staining. Astrocytes were

transfected with a myc-tagged expression vector of ROCK-I-Δ1 and visualized in red (anti-myc), blue (Hoechst) and green (TUNEL). Our results showed that active ROCK-I induced DNA fragmentation that overlaps with the chromatin condensation (Hoechst staining) (Fig. 4E). Statistical analysis showed that ROCK-I-Δ1 induced a significant increase in both membrane blebbing and chromatin condensation (Fig. 4F). These results indicate that both RhoA and ROCK-I induce the

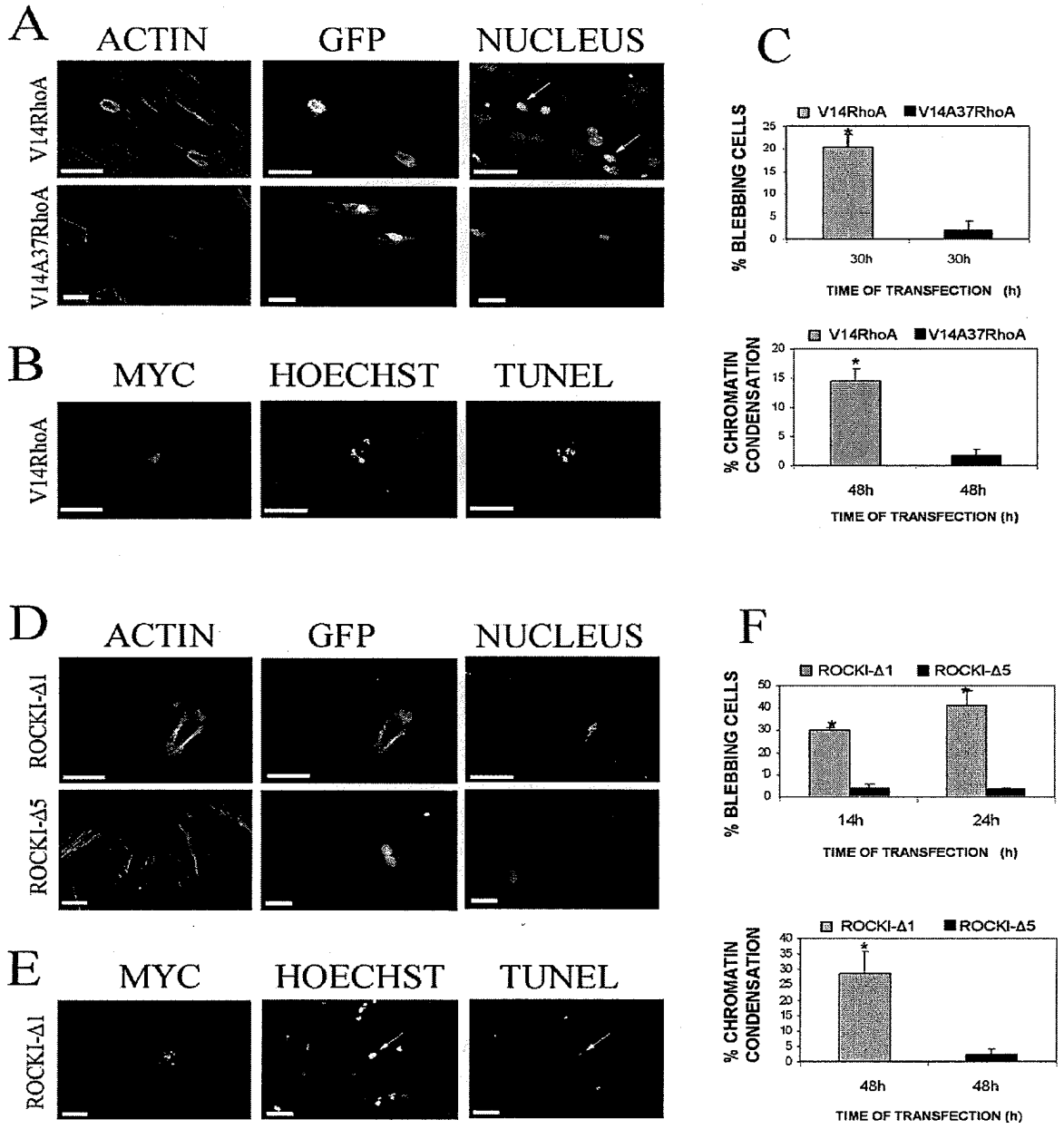

Fig. 4. RhoA and ROCK-I induce membrane blebbing, chromatin condensation and DNA framentation. (A,D) Cultured astrocytes were grown for seven days and then cotransfected with plasmids expressing either active proteins (V14RhoA and ROCKI-Δ1) or inactive proteins (V14A37RhoA and ROCKI-Δ5) together with a plasmid expressing GFP. Astrocytes transfected with either RhoA (A) or ROCK-I (D) were analyzed by immunofluorescence (actin, GFP and nuclear condensation). (B,E) Active proteins (V14RhoA and ROCKI-Δ1) induce DNA fragmentation as revealed by TUNEL staining (green) in astrocytes transfected with myc-tagged expression vectors of either V14RhoA (B) or ROCK-I (E). (C) Quantification of blebbing cells, as well as chromatin condensation (Hoechst staining), in astrocytes overexpressing either RhoA (C) or ROCK-I (F). Values are mean ±s.d. of five different experiments. *$P<0.001$ versus control values in one-way ANOVA. Bars, 10 μm.

formation of stress fibres, which probably drives cell contraction, resulting in membrane blebbing and chromatin condensation in astrocytes.

Activation of ROCK-I by RhoA, rather than by caspase-3, participates in the ethanol-induced apoptosis

ROCK-I can control blebbing either after its activation by RhoA or as a result of caspase-3 cleavage (Sebbagh et al., 2001). Therefore, we wondered whether ROCK-I is implicated in the apoptotic process induced by ethanol, and which molecules activate ROCK-I in this process. To answer these questions, we used ethanol-treated astrocytes (100 mM) at different times of ethanol exposure (3-24 hours) and the ROCK-I kinase activity was measured after its immunoprecipitation with either the H-85 or C-19 antibody. The H-85 antibody recognizes amino acids 755-840 mapping within an internal region of ROCK-I, therefore it binds both the full-length p160ROCK-I and the caspase-3-cleaved constitutively active p130ROCK-I. However, C-19 is a specific antibody against the C-termini of ROCK-I, and only binds to the full-length p160ROCK-I molecule (Sebbagh et al., 2001). Indeed, a western blot analysis of the control lysates immunoprecipitated with C-19 revealed that this antibody precipitated p160ROCK-I, but not p130ROCK-I (Fig. 5C). This figure also showed that RhoA co-immunoprecipitated with the full-length p160ROCK-I.

When ROCK-I kinase activity was measured in lysates of astrocytes (control or ethanol-treated), that were previously immunoprecipitated with either C-19 or H-85 antibody, we observed that ethanol treatment induced an activation of this kinase, when compared with control astrocytes. Furthermore, this increase in the ROCK-I kinase activity induced by ethanol was similar when either C-19 or H-85 was used for the inmmunoprecipitation (Fig. 5A). Because H-85 recognized both the p160ROCK-I and p130ROCK-I, while C-19 only recognized p160ROCK-I, these results indicate that ethanol most probably activates ROCK-I through the RhoA binding, and also suggest that caspase-mediated ROCK-I activation does not participate in this process.

To support this hypothesis further, ethanol-treated astrocytes were subjected to a pull-down assay with GST-TRBD (Rho-binding domain from Rhotekin, one of the Rho effectors) to affinity precipitate endogenous GTP-Rho (Ren et al., 1999). This domain should bind only GTP-Rho and inhibits its conversion to the GDP state, therefore the amount of Rho retained on TRBD beads should provide a measure of Rho-GTP loading (Ren and Schwartz, 2000). Our results showed that ethanol treatment induced activation of RhoA that is maximal at 6 hours of ethanol treatment (Fig. 5B). In addition, immunoprecipitation with C-19 and western blot analysis showed that ethanol exposure induced an increase in the levels of RhoA that were bound to ROCK-I (Fig. 5C). We also observed a correlation between the highest RhoA levels and the maximum ROCK-I activity at 14 hours (Fig. 5A), although this correlation was not observed in the case of RhoA activation. Interaction of RhoA with ROCK could lead to the kinase activation in a nucleotide-independent manner and would explain the decrease of RhoA activation at 14 hours. Indeed, a new Rho binding domain of ROCK (HR1), that binds RhoA in a nucleotide-independent manner, has been recently demonstrated (Blumenstein and Ahmadian, 2004).

In addition, preincubation of astrocytes with the RhoA inhibitor C3, when using either the C-19 or H-85 antibody for the immunoprecipitation, resulted in the abrogation of the ethanol-induced ROCK-I activation (Fig. 5D). Notably, our results also suggest that caspase-mediated ROCK-I activation does not participate in this process, as ethanol exposure did not induce an increase in the levels of the caspase-3-cleaved p130ROCK-I in astrocyte lysates, as demonstrated by western blot analysis when H-85 antibody was used (Fig. 5E-a). We then tested whether other caspase-3 substrates, such as poly (ADP-ribose) polymerase (PARP), were cleaved during ethanol treatment. Fig. 5E-b illustrates a cleavage form of PARP in astrocytes treated with ethanol, supporting the notion of caspase-3 cleaving PARP and not ROCK-I.

We also noted that the ROCK-I kinase activity increased at 6 hours of ethanol treatment, it peaked at 14 hours and it reached baseline values at 24 hours (Fig. 5A). These results are in accordance with the highest caspase-3 activity after a 14-hours ethanol treatment (Fig. 1A), suggesting that ROCK-I is involved in ethanol-induced apoptosis. Therefore, inhibition of either ROCK or RhoA should lead to the abrogation of the apoptotic process induced by ethanol. Indeed, preincubation of astrocytes with either Y-27632, an inhibitor of ROCK activity (Coleman et al., 2001; Ishizaki et al., 2000; Sebbagh et al., 2001) or C3, inhibitor of Rho (Ridley and Hall, 1992) before ethanol treatment, totally prevented the ethanol-induced membrane blebbing at all times tested (Fig. 5F), as well as cell rounding and chromatin condensation (data not shown). We also observed a partial inhibition of the caspase-3 activity when astrocytes were pretreated with either Y-27632 or C3 and then exposed to ethanol for different times (Fig. 5G). Interestingly, ROCK inhibition did not affect the annexin-V staining (Fig. 5H), as previously demonstrated in 'bona fide' apoptotic cells (Cocca et al., 2002).

These results, together with the findings indicating that both RhoA and ROCK-I induce blebbing, strongly support the conclusion that RhoA/ROCK-I pathway is implicated in the appearance of ethanol-induced membrane blebbing in astrocytes.

MLC is phosphorylated during the ethanol-induced apoptosis

ROCK contributes to actin-myosin force generation, causing blebs to protrude through MLC phosphorylation (MLC-pp) (Coleman and Olson, 2002). Therefore, we then addressed the question whether ethanol induced an increase in MLC phosphorylation. Astrocytes were exposed to ethanol (100 mM) at different times (3-24 hours) and MLC phosphorylation was investigated in immunoprecipitates using specific antibodies against MLC-pp. Western blot analysis showed that ethanol induced an increase in MLC phosphorylation in astrocytes. This increase was observed within 14 hours of ethanol exposure and it declined at 24 hours (Fig. 6). It is interesting to note that MLC-pp pattern correlated with the kinetics of ethanol-induced ROCK-I activation. To further demonstrate that MLC phosphorylation is downstream of RhoA/ROCK pathway during the ethanol-induced apoptosis, astrocytes were treated with ethanol in the presence of either Y-27632 or C3. Our results demonstrated that both inhibitors considerably reduced the ethanol-induced MLC-pp at different times of the treatment. These results support that the

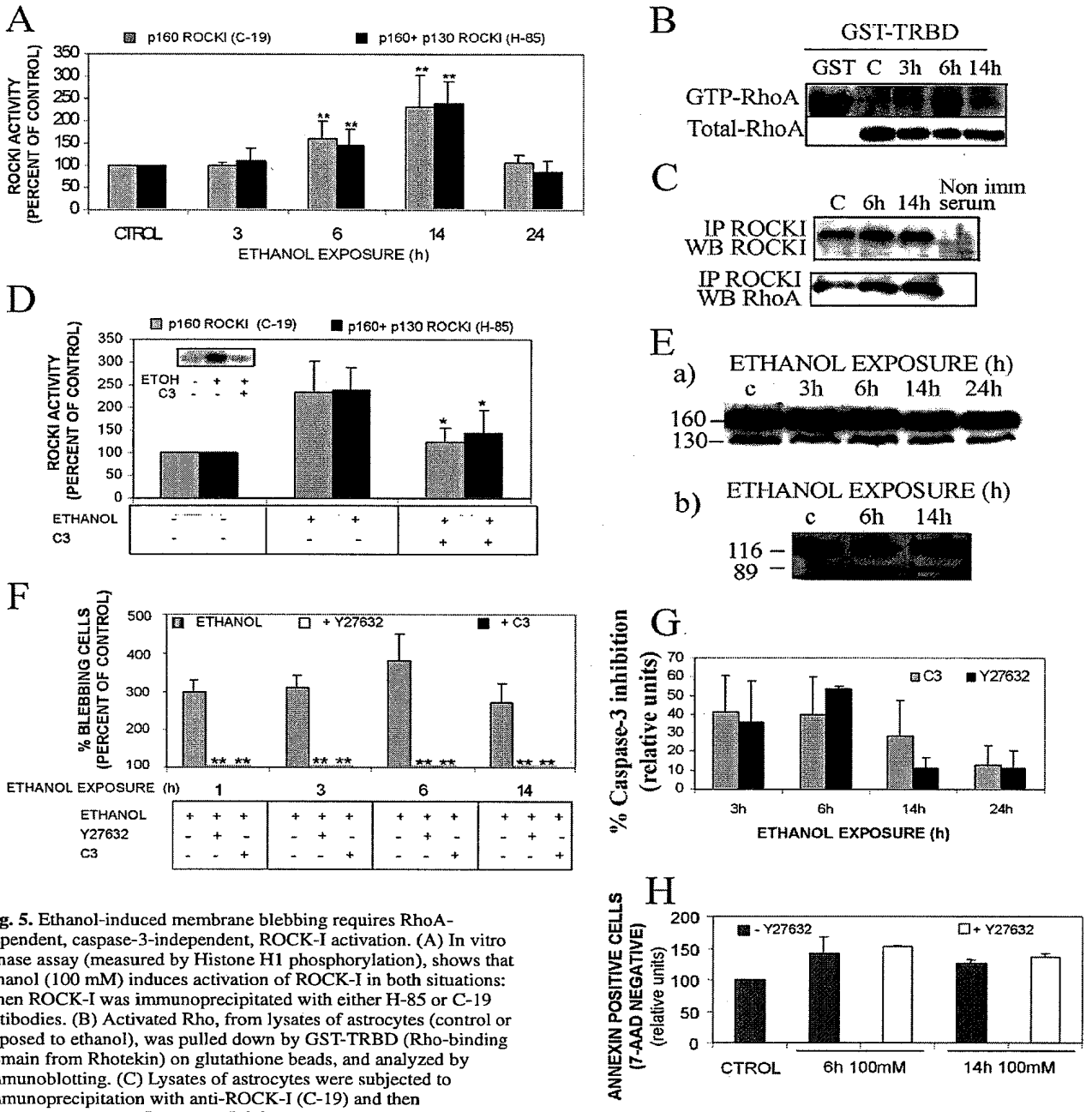

Fig. 5. Ethanol-induced membrane blebbing requires RhoA-dependent, caspase-3-independent, ROCK-I activation. (A) In vitro kinase assay (measured by Histone H1 phosphorylation), shows that ethanol (100 mM) induces activation of ROCK-I in both situations: when ROCK-I was immunoprecipitated with either H-85 or C-19 antibodies. (B) Activated Rho, from lysates of astrocytes (control or exposed to ethanol), was pulled down by GST-TRBD (Rho-binding domain from Rhotekin) on glutathione beads, and analyzed by immunoblotting. (C) Lysates of astrocytes were subjected to immunoprecipitation with anti-ROCK-I (C-19) and then immunoblotted with RhoA and ROCK-I (C19) antibodies. (D) Inhibition of ROCK-I kinase activity using C3 exoenzyme in control- and ethanol-exposed astrocytes (100 mM) (see Materials and Methods). $*P<0.05$ versus ethanol-treated cells in a one-way ANOVA. (E-a) A representative western blotting of ROCK-I using H-85 antibody is shown, in control and ethanol-treated astrocytes. (E-b) A representative western blot analysis of PARP cleavage in astrocytes exposed to ethanol (100 mM) for 6 and 14 hours. (F) Ethanol-induced blebbing is abolished when cells are pretreated with either Y-27632 (a ROCK inhibitor) or C3 exoenzyme (a Rho inhibitor). $**P<0.001$ versus ethanol-treated experiments in a one-way ANOVA. (G) Preincubation of astrocytes with either Y-27632 or C3 before ethanol treatment (3, 6, 14 and 24 hours) decreases the caspase-3 activity. Percent of caspase-3 inhibition was calculated by comparing the activity in the presence and absence of the inhibitor, at each time-point analyzed. Results are mean ±s.d. of three different experiments. (H) Quantification of annexin-V positive cells (7-AAD^-) of ethanol-exposed astrocytes, in the presence and absence of the ROCK inhibitor Y-27632. Results are the average of around 500 cells from three different cultures. Values are mean ±s.d. of five different experiments. $*P<0.05$ and $**P<0.001$ versus control values in one-way ANOVA.

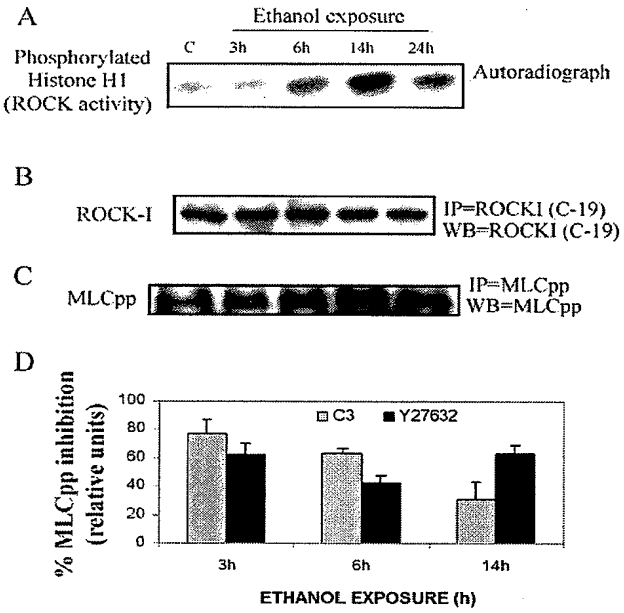

Fig. 6. Ethanol-induced MLC phosphorylation correlates with ROCK-I kinase activity. Cultured astrocytes were treated with 100 mM alcohol for 3, 6, 14 and 24 hours. Lysates of control and ethanol-treated astrocytes were subjected to immunoprecipitation with the anti-ROCK-I antibody C-19. These immunoprecipitates were used for A and B. (A) ROCK-I kinase activity measured by phosphorylated Histone H1. A representative autoradiograph is shown. (B) Western blot analysis of ROCK-I, as a control of protein content. (C) A representative western blotting of phosphorylated MLC from lysates of astrocytes (control and ethanol-treated) that were immunoprecipitated with anti-MLC-pp antibody. (D) Inhibition of the ethanol-induced MLC phosphorylation when astrocytes are pretreated with either Y27632 or C3. Bars represent the mean ±s.d. of the densitometric quantification obtained from three different immunoblots. Percent of MLCpp inhibition was calculated by comparing the densitometric values in the presence and absence of the inhibitor, at each time-point analyzed.

RhoA/ROCK-I/MLC pathway is involved in ethanol-induced apoptosis.

Discussion

Anoikis is a programmed cell death induced by the loss of cell-matrix interactions and plays a physiological role by regulating cell homeostasis in tissues. However, anoikis can also be involved in pathological processes as demonstrated by the resistance to anoikis in cancer and its enhancement in degenerative tissue remodeling (Grossmann, 2002), such as the cardiac myocyte detachment in heart failure (Michel, 2003). We have recently shown that ethanol profoundly disorganizes the actin cytoskeleton in astrocytes leading to the formation of peripheral actin rings, the disappearance of stress fibres and a decrease in the content of focal adhesions (Guasch et al., 2003). Interestingly, these features mimic those observed during the execution phase of apoptosis, including cell detachment from the extracellular matrix as well as the reorganization of focal adhesion, adopting a 'rounded' morphology, a process named anoikis (Mills et al., 1999). Therefore, we decided to analyze whether ethanol-induced actin rings along with both a reduction and a reorganization of focal adhesions could be an initial step in an anoikis process. In addition, since small Rho GTPases have been implicated in actin cytoskeleton organization (Ridley and Hall, 1992) and apoptosis (Mills et al., 1998), we also assessed the potential role that the RhoA signalling pathway plays in the morphological changes associated with the ethanol-induced apoptosis. Here we show that astrocytes undergo apoptosis by anoikis when exposed to ethanol and that this process is mediated by the RhoA/ROCK-I/MLC pathway.

We have previously shown that ethanol exposure during the cerebral cortex development increases astrocytic cell death (Climent et al., 2002). The present results also show that ethanol can induce apoptosis in astrocytes in culture, as demonstrated by the annexin-V/7AAD staining, propidium iodide labelling and caspase-3 activity. Indeed, by using propidium iodide labelling followed by flow cytometry analysis, as one of the best quantitative techniques to detect apoptosis in astrocytes (Micoud et al., 2001), we demonstrate that ethanol dose-dependently increases both the apoptotic sub-G0/G1 peak (a characteristic cell population with a lower DNA content than the normal cells have) (Lizard et al., 1996) and the caspase-3 activity. These findings indicate that astrocytes undergo apoptosis when exposed to ethanol and that this cell death is detected as early as 3 hours of 100 mM ethanol exposure.

It is known that cells undergo several morphological changes during apoptosis, including cell contraction, dynamic membrane blebbing and chromatin condensation (Mills et al., 1999). These events, which represent the evolutionarily conserved execution phase of apoptosis, require sequential changes in cell-matrix interaction and actin cytoskeleton, that lead to the cell detachment from the extracellular matrix and to fragmentation into small apoptotic bodies (Mills et al., 1999). In accordance with these findings, our results demonstrate that these alterations also occur in ethanol-treated astrocytes. Indeed, we observe that ethanol induces actin-myosin peripheral reorganization, membrane blebbing and chromatin condensation.

However, apoptosis can be induced by the loss of anchorage, a process termed anoikis that represents a direct entry into the release stage. It is characterized by both disassemble and peripheral reorganization of the focal adhesion proteins, where a rounded morphology is adopted (Mills et al., 1999). During this process dephosphorylation of the focal adhesion proteins, such as paxillin and FAK, also occurs (Bannerman et al., 1998; van de Water et al., 1999). Our results show that ethanol decreases the content and also relocalizes paxillin (a focal adhesion protein) along with a peripheral actin-myosin reorganization in the rounded cell body. Likewise, ethanol-treated cells display a marked reduction in the phosphotyrosine levels, detected as early as 15 minutes of ethanol treatment. These findings suggest that ethanol induces cell death by anoikis, since we observe a loss of membrane attachments along with peripheral reorganization of the actin-myosin that contracts the cell body and leads to bleb formation.

Previous studies have demonstrated that the first stage of cell contraction during the apoptotic process depends upon the

presence of the filamentous actin, whereas the second phase involves actin disassembly (Suarez-Huerta et al., 2000). Since RhoA regulates actin organization, promotes actin-myosin contractile force (Coleman and Olson, 2002) and activates the effector ROCK-I (Ishizaki et al., 1997), we asked whether the RhoA/ROCK-I signalling pathway was implicated in the ethanol-induced apoptosis. We demonstrated that either V14RhoA or active ROCK-I is sufficient to induce membrane blebbing, chromatin condensation and DNA fragmentation in cultured astrocytes. Furthermore, we also showed that ethanol treatment induces a substantial activation of ROCK-I that correlates with the higher levels of apoptosis. Indeed, maximum levels of both ROCK-I activation and apoptosis were observed at a 14 hours ethanol exposure. The involvement of ROCK-I in the ethanol-induced apoptosis is further supported by the experiment showing that inhibition of ROCK with Y-27632 totally prevented the ethanol-induced apoptotic blebbing. In fact, it has been previously shown that inhibition of ROCK-I strongly decreases apoptotic blebbing, but has no effect on necrotic blebbling (Barros et al., 2003).

Interaction of Rho with ROCK-I results in an open conformation of the kinase that frees the catalytic activity. In addition, ROCK-I can be activated by caspase-3-mediated cleavage (Coleman et al., 2001; Sebbagh et al., 2001). Furthermore, some studies suggest that ROCK-I could control bleb formation either after it is cleaved by caspase-3 or as a result of sustained Rho activation (Sebbagh et al., 2001). By using two antibodies that recognize either the full-length p160ROCK-I (C-19) or both the full-length and the caspase-3-cleaved p130ROCK-I (H-85), we demonstrate that astrocytes exposed to ethanol show a similar increase in the ROCK-I kinase activity when these cells were immunoprecipitated either with C-19 or with H-85. These results suggest that RhoA, rather than caspase-3, participates in the ethanol-induced ROCK-I activation.

This hypothesis is further supported by the following findings: first, ethanol treatment induces RhoA activation. Second, preincubation with the C3 toxin, that inactivates Rho, completely abolishes both kinase activities (with either C-19 or H-85 antibody). Third, immunoprecipitation with C-19 and western blotting analysis demonstrate a correlation between higher levels of RhoA and the highest ROCK-I activity. Fourth, the ethanol-induced bleb formation, which is mediated by ROCK-I, was prevented by the toxin C3, a RhoA inhibitor. Fifth, ethanol-treated astrocytes show no increasing levels of the caspase-3-cleaved p130ROCK-I molecule, at each ethanol treatment tested. Interestingly, another caspase-3 substrate, such as PARP, is cleaved in astrocytes exposed to ethanol. Taken together, all these results strongly support the hypothesis that ROCK-I is activated by RhoA in ethanol-treated astrocytes, where the participation of the caspase-3-cleaved ROCK-I is unlikely.

Activation of ROCK can also induce MLC phosphorylation, contributing to the actin-myosin force generation that is necessary for cell contraction and membrane blebbing (Coleman and Olson, 2002). Indeed, several reports indicate that ROCK directly phosphorylates MLC (Amano et al., 1996; Kureishi et al., 1997) and also inhibits MLC phosphatase by phosphorylation (Kawano et al., 1999; Kimura et al., 1996). We observe that ethanol markedly increases MLC-pp, that peaks at 14 hours of ethanol incubation and it declined thereafter. This MLC-pp pattern was seen to correlate with the kinetics of the activation of ROCK-I by ethanol. Indeed, previous results have demonstrated that ROCK-I induces MLC phosphorylation (Sebbagh et al., 2001). Taken together, these findings indicate that MLC phosphorylation is downstream of RhoA/ROCK-I pathway, since inhibition of either ROCK or RhoA leads to a significant decrease in the ethanol-induced MLC-pp. Our data also suggest that ROCK-I induced MLC phosphorylation participates in the ethanol-induced cell contraction and membrane blebbing.

To summarise, our results demonstrate that astrocytes undergo apoptosis by anoikis when exposed to ethanol and suggest that this process is mediated by the activation of the RhoA/ROCK-I/MLC pathway, leading to acto-myosin contraction and membrane blebbing. In addition, our results suggest that the activation of ROCK-I by caspase-3 does not participate in the ethanol-induced apoptosis. These findings provide the first evidence that ethanol can cause cell death by anoikis and suggest that alterations in actin cytoskeleton organization may underlie the ethanol-induced astroglial death during brain development (Climent et al., 2002). These findings may contribute to unravel the mechanisms involved in the CNS alterations observed in brains of children with foetal alcohol syndrome.

Materials and Methods

Astrocyte culture

Primary cultures of astrocytes from 21-day-old rat fetuses were prepared from brain hemispheres as described in detail previously (Renau-Piqueras et al., 1989). The purity of astrocyte cultures was assessed by immunofluorescence using a mouse anti-GFAP monoclonal antibody (Sigma-Aldrich). In our conditions, 99% of the cells were astrocytes. Cells were used after 7-10 days of culture.

For ethanol exposure, astrocytes were treated with 100 mM ethanol for 3, 6, 14 or 24 hours. The alcohol concentration used are in the range of the blood alcohol levels found among alcoholics (BAL 51-106 mM) (Jones and Sternebring, 1992).

Apoptosis quantification

Astrocytes treated with 100 mM and 200 mM of ethanol for different times (3, 6, 14 and 24 hours) were used and apoptosis was quantified by three methods: sub-G0/G1 population, caspase-3 activity and annexin-V/7-AAD (7-amino-actinomycin D).

For the analysis of sub-G0/G1 population, astrocytes were fixed with ethanol 80% for 30 minutes at –20°C, followed by incubation in a solution of 50 μM propidium iodide containing 250 μg/ml RNAse A for 20 minutes. For the sub-G0/G1 inhibition studies, cells were preincubated with 100 μM z-VAD-fmk (Sigma-Aldrich) for 2 hours before the ethanol treatment and analyzed with an EPICS XL flow cytometer. WinMDI and Cylchred software were used to analyze DNA content.

Caspase-3 activity was measured by a colourimetric assay kit (Sigma-Aldrich) according to the manufacturer's instructions. Caspase-3 activity was also assessed using three inhibitors: z-VAD-fmk (50 μM or 100 μM), C3 exoenzyme (Calbiochem) and Y-27632, a ROCK inhibitor (Santa Cruz Biotechnology). For z-VAD-fmk and Y-27632 treatments, astrocytes were pre-incubated with these inhibitors 2 hours before the ethanol exposure. For C3 treatment, astrocytes were transfected with 5 μg of C3 (precomplexed with 3 μl of FuGENE 6 Reagent in 100 μl of DMEM), 3 hours before ethanol exposure.

To analyze apoptosis further and to differentiate between apoptosis and necrosis, cells were labelled with R-phycoerythrin-conjugated annexin-V in combination with the cell-impermeant DNA fluorophore 7-AAD (both Molecular Probes). The assay was performed according to the manufacturer's protocol. For the inhibition studies, astrocytes were preincubated with Y-27632 (10 μM) for 2 hours before the ethanol treatment. Cells were analyzed with an EPICS XL flow cytometer.

Transfections

Cortical astrocytes were seeded on 16 mm glass coverslips and transfected when still subconfluent. Cells were cotransfected with FuGENE™ 6 (Roche Diagnostics) according to the manufacturer's protocol. Plasmid DNA consisted of 1 μg of either pCAG-ROCK-I-Δ1 or pCAG-ROCK-I-Δ5 (Ishizaki et al., 1997) together with 0.1 μg of GFP to identify transfected astrocytes. For RhoA studies, 1 μg of either pEXV3-V14RhoA or pEXV3-V14A37RhoA together wth 0.1 μg of GFP were used. For TUNEL staining, astrocytes were transfected with myc-tagged expression vectors of V14RhoA (pEXV3-V14RhoA) and ROCK-I-Δ1 (pCAG-

ROCK-I-Δ1). Under our experimental conditions, transfection efficiency was ≅7% and at least 200 transfected cells from four different cultures were analyzed for each experiment.

Fluorescence microscopy

Astrocytes growing on 16 mm glass coverslips were used for immunofluorescence analysis. Cells were fixed and permeabilized as previously described (Guasch et al., 2003). For actin-myosin colocalization, cells were incubated with anti-myosin IIA (non-muscle) (1:200; Sigma) followed by incubation with FITC-conjugated goat anti-rabbit IgG (1:200; Sigma). For the ROCK inhibition studies, ROCK inhibitor (Y-27632) (Santa Cruz Biotechnology, Madrid, Spain) was used at 10 μM with an hour pre-treatment. For endogenous RhoA inhibition, C3 exoenzyme (Calbiochem) was transfected in astrocytes. For transfection, 2.5 μg of C3 were pre-complexed with 3 μl of FuGENE 6 Reagent in 100 μl of DMEM and complexes were added to the coverslips after 30 minutes of incubation at room temperature. Thereafter, ethanol treatments were performed.

Focal adhesions were stained with anti-paxillin (1:200; Transduction Laboratories) followed by incubation with FITC-conjugated goat anti-mouse IgG antibody (1:200; Jackson Immunoresearch). Phosphotyrosine residues were studied using an anti-phosphotyrosine antibody, clone 4G10 (1:200; Upstate Biotechnology) followed by FITC-conjugated goat anti-mouse IgG. Cellular nuclei were detected by incubation with Hoechst (1:20,000; Molecular Probes). Micrographs were digitally recorded with a Zeiss microscope (Axioskop 2, Zeiss).

DNA fragmentation was analyzed by using the In Situ Cell Death Detection Kit, Fluorescein (Roche Diagnostics). Astrocytes were transfected with either ROCK-I or RhoA plasmids. The TUNEL reaction was performed according to the manufacturer's protocol. For myc detection, the anti-9E10 antibody was used (1:200; Santa Cruz Biotechnology), followed by a TRITC-conjugated goat anti mouse IgG antibody (1:100; Jackson ImmunoResearch).

Immunoprecipitation, western blotting and kinase assay

For immunoblot studies cells were lysed in lysis buffer (1% NP40, 20 mM Tris-HCl, pH 8, 130 mM NaCl, 10 mM NaF, 10 μg/ml aprotinin, 40 μM leupeptin, 1 mM DTT, 1 mM Na_3VO_4 and 1 mM PMSF) by incubating for 30 minutes on ice. Then, proteins were electrophoresed on SDS-PAGE, transferred to PVDF membranes and incubated for 1 hour with the following antibodies: anti-paxillin (1:1000, Transduction Laboratories), anti-RhoA (1:500, Santa Cruz Biotechnologies), anti-Thr18/Ser19 MLCpp (1:1000, Santa Cruz Biotechnology) and anti-PARP (1:500, Cell Signalling). For ROCK-I detection, two different antibodies were used: goat polyclonal anti ROCK-I (C-19, sc-6055) (1:100), which is raised against a peptide mapping at the C-terminus of ROCK-I; and rabbit polyclonal anti ROCK-I (H-85, sc-5560) (1:500), which recognizes amino acids 755-840 mapping within an internal region of ROCK-I (both purchased by Santa Cruz Biotechnology). After washing in TBS-Tween, blots were incubated with horseradish peroxidase-conjugated antibodies: anti-mouse IgG (1:1000; Santa Cruz Biotechnology) for paxillin and RhoA; anti-rabbit (1:20,000; Sigma-Aldrich) for H-85 and PARP; anti-goat (1:20,000; Sigma) for both ROCK-I (C-19) and MLCpp. Finally, blots were developed using the enhanced chemiluminescence system (ECL Plus, Amersham Pharmacia Biotech).

For the immunoprecipitation studies, lysates were precleared by addition of protein A/G PLUS-agarose beads (Santa Cruz Biotechnology) (10 μl agarose beads per 100 μg cell protein), and then incubated overnight with specific antibodies (1 μg per 100 μg cell protein) together with the suitable amount of protein A/G PLUS-agarose beads (10 μl agarose beads per 100 μg cell protein). Proteins were immunoblotted as described above. Non-immune serum was used as a control to discard non-specific interactions. To detect MLCpp, 200 μg of cell protein were immunoprecipitated using 1 μg of anti-Thr18/Ser19 MLCpp antibody and western blotting was performed as previously described. Astrocytes were pretreated with either C3 (5 μg/ml together with 3 μl/ml of FuGENE 6) or Y-27632 (10 μM), before ethanol exposure (100 mM for 3, 6 and 14 hours).

To analyze the direct interaction between ROCK-I and RhoA, cell supernatants were incubated for 2 hours with anti-ROCK-I polyclonal (C-19) antibody and RhoA western blotting was performed. To detect ROCK-I, membranes were stripped and then ROCK-I was detected with anti-ROCK-I polyclonal (C-19), as previously described. Non-immune goat serum (diluted 1:10,000) was also used as a control to discard non-specific interactions.

For ROCK-I kinase assays, 400 μg of cell lysates were incubated overnight either with anti-ROCK-I (C-19) or with anti-ROCK-I (H-85) together with agarose beads, as already described. The kinase assay was performed in 30 μl of kinase buffer containing 15 μg Histone H1 (Roche Diagnostics), 30 μM ATP (Sigma-Aldrich) and 5 μCi [γ-^{32}P]ATP (Amersham Pharmacia Biotech.) for 30 minutes at 30°C. Radiolabelled Histone H1 was resolved by SDS-PAGE and the gel was dried and subjected to autoradiograph.

Inhibition of endogenous RhoA was performed using Clostridium Botulinum C3 transferase exoenzyme. Astrocytes were transfected with 5 μg/ml of C3 Exoenzyme (Calbiochem, Madrid, Spain) and 3 μl/ml of FuGENE 6 (Roche Diagnostics). After a 3 hour preincubation with C3 exoenzyme, ethanol (100 mM) was added for 14 hours.

RhoA pull-down assay

RhoA activity was measured with recombinant purified GST-TRBD (GST-rhotekin Rho-binding domain) bound to glutathione beads (Amersham Biosciences). GST and GST-TRBD (a gift from M. Schwartz, Scripps Institute, San Diego, CA) were expressed in *Escherichia coli* and purified as previously described (Ren and Schwartz, 2000). Lysates were incubated with 30 μg of GST or GST-TRBD beads for 1 hour at 4°C. Proteins retained on the GST-TRBD beads were resolved by 13% SDS-PAGE. Bound RhoA was detected by western blot using anti-RhoA antibody (Santa Cruz) and developed by chemiluminescence.

We gratefully acknowledge Anne J. Ridley for the generous gift of V14RhoA and V14A37RhoA plasmids, Shuh Narumiya for ROCK-I-Δ1 and ROCK-I-Δ5 and Martin Schwartz for the GST-TRBD. We also thank J. E. O'Connor for his assistance with FACS analysis and M. March and M. C. García-Minguillán for their excellent technical help. This research was supported by grants from MCYT (BFI 2001-0123; SAF 2003-06217), Instituto de Salud Carlos III (CP03/00105), Red RTA (G03/005) and Generalitat Valenciana.

References

Amano, M., Ito, M., Kimura, K., Fukata, Y., Chihara, K., Nakano, T., Matsuura, Y. and Kaibuchi, K. (1996). Phosphorylation and activation of myosin by Rho-associated kinase (Rho-kinase). *J. Biol. Chem.* **271**, 20246-20249.

Amano, M., Chihara, K., Kimura, K., Fukata, Y., Nakamura, N., Matsuura, Y. and Kaibuchi, K. (1997). Formation of actin stress fibres and focal adhesions enhanced by Rho-kinase. *Science* **275**, 1308-1311.

Anthony, T. E., Klein, C., Fishell, G. and Heintz, N. (2004). Radial glia serve as neuronal progenitors in all regions of the central nervous system. *Neuron* **41**, 881-890.

Aschner, M., Allen, J. W., Kimelberg, H. K., LoPachin, R. M. and Streit, W. J. (1999). Glial cells in neurotoxicity development. *Annu. Rev. Pharmacol. Toxicol.* **39**, 151-173.

Bannerman, D. D., Sathyamoorthy, M. and Goldblum, S. E. (1998). Bacterial lipopolysaccharide disrupts endothelial monolayer integrity and survival signaling events through caspase cleavage of adherens junction proteins. *J. Biol. Chem.* **273**, 35371-35380.

Barros, L. F., Kanaseki, T., Sabirov, R., Morishima, S., Castro, J., Bittner, C. X., Maeno, E., Ando-Akatsuka, Y. and Okada, Y. (2003). Apoptotic and necrotic blebs in epithelial cells display similar neck diameters but different kinase dependency. *Cell Death Differ.* **10**, 687-697.

Blumenstein, L. and Ahmadian, M. R. (2004). Models of the cooperative mechanism for Rho effector recognition: implications for RhoA-mediated effector activation. *J. Biol. Chem.* **279**, 53419-53426.

Burridge, K. and Wennerberg, K. (2004). Rho and Rac take center stage. *Cell* **116**, 167-179.

Chrzanowska-Wodnicka, M. and Burridge, K. (1996). Rho-stimulated contractility drives the formation of stress fibers and focal adhesions. *J. Cell Biol.* **133**, 1403-1415.

Climent, E., Pascual, M., Renau-Piqueras, J. and Guerri, C. (2002). Ethanol exposure enhances cell death in the developing cerebral cortex: role of brain-derived neurotrophic factor and its signaling pathways. *J. Neurosci. Res.* **68**, 213-225.

Cocca, B. A., Cline, A. M. and Radic, M. Z. (2002). Blebs and apoptotic bodies are B cell autoantigens. *J. Immunol.* **169**, 159-166.

Coleman, M. L. and Olson, M. F. (2002). Rho GTPase signalling pathways in the morphological changes associated with apoptosis. *Cell Death Differ.* **9**, 493-504.

Coleman, M. L., Sahai, E. A., Yeo, M., Bosch, M., Dewar, A. and Olson, M. F. (2001). Membrane blebbing during apoptosis results from caspase-mediated activation of ROCK I. *Nat. Cell Biol.* **3**, 339-345.

Costa, L. G., Aschner, M., Vitalone, A., Syversen, T. and Soldin, O. P. (2004). Developmental neuropathology of environmental agents. *Annu. Rev. Pharmacol. Toxicol.* **44**, 87-110.

Crespel, A., Coubes, P., Rousset, M. C., Alonso, G., Bockaert, J., Baldy-Moulinier, M. and Lerner-Natoli, M. (2002). Immature-like astrocytes are associated with dentate granule cell migration in human temporal lobe epilepsy. *Neurosci. Lett.* **330**, 114-118.

Doetsch, F. (2003). The glial identity of neural stem cells. *Nat. Neurosci.* **6**, 1127-1134.

Eriksen, J. L. and Druse, M. J. (2001). Astrocyte-mediated trophic support of developing serotonin neurons: effects of ethanol, buspirone, and S100B. *Brain Res. Dev. Brain Res.* **131**, 9-15.

Fields, R. D. and Stevens-Graham, B. (2002). New insights into neuron-glia communication. *Science* **298**, 556-562.

Grossmann, J. (2002). Molecular mechanisms of 'detachment-induced apoptosis–Anoikis'. *Apoptosis* **7**, 247-260.

Guasch, R. M., Tomas, M., Minambres, R., Valles, S., Renau-Piqueras, J. and Guerri, C. (2003). RhoA and lysophosphatidic acid are involved in the actin cytoskeleton reorganization of astrocytes exposed to ethanol. *J. Neurosci. Res.* **72**, 487-502.

Guerri, C. (2002). Mechanisms involved in central nervous system dysfunctions induced by prenatal ethanol exposure. *Neurotox. Res.* **4**, 327-335.

Guerri, C. and Renau-Piqueras, J. (1997). Alcohol, astroglia, and brain development. *Mol. Neurobiol.* **15**, 65-81.

Herault, O., Colombat, P., Domenech, J., Degenne, M., Bremond, J. L., Sensebe, L., Bernard, M. C. and Binet, C. (1999). A rapid single-laser flow cytometric method

for discrimination of early apoptotic cells in a heterogenous cell population. *Br. J. Haematol.* **104**, 530-537.

Huot, J., Houle, F., Rousseau, S., Deschesnes, R. G., Shah, G. M. and Landry, J. (1998). SAPK2/p38-dependent F-actin reorganization regulates early membrane blebbing during stress-induced apoptosis. *J. Cell Biol.* **143**, 1361-1373.

Ishizaki, T., Maekawa, M., Fujisawa, K., Okawa, K., Iwamatsu, A., Fujita, A., Watanabe, N., Saito, Y., Kakizuka, A., Morii, N. et al. (1996). The small GTP-binding protein Rho binds to and activates a 160 kDa Ser/Thr protein kinase homologous to myotonic dystrophy kinase. *EMBO J.* **15**, 1885-1893.

Ishizaki, T., Naito, M., Fujisawa, K., Maekawa, M., Watanabe, N., Saito, Y. and Narumiya, S. (1997). p160ROCK, a Rho-associated coiled-coil forming protein kinase, works downstream of Rho and induces focal adhesions. *FEBS Lett.* **404**, 118-124.

Ishizaki, T., Uehata, M., Tamechika, I., Keel, J., Nonomura, K., Maekawa, M. and Narumiya, S. (2000). Pharmacological properties of Y-27632, a specific inhibitor of rho-associated kinases. *Mol. Pharmacol.* **57**, 976-983.

Jones, A. W. and Sternebring, B. (1992). Kinetics of ethanol and methanol in alcoholics during detoxification. *Alcohol Alcohol.* **27**, 641-647.

Kawano, Y., Fukata, Y., Oshiro, N., Amano, M., Nakamura, T., Ito, M., Matsumura, F., Inagaki, M. and Kaibuchi, K. (1999). Phosphorylation of myosin-binding subunit (MBS) of myosin phosphatase by Rho-kinase in vivo. *J. Cell Biol.* **147**, 1023-1038.

Kimura, K., Ito, M., Amano, M., Chihara, K., Fukata, Y., Nakafuku, M., Yamamori, B., Feng, J., Nakano, T., Okawa, K. et al. (1996). Regulation of myosin phosphatase by Rho and Rho-associated kinase (Rho-kinase). *Science* **273**, 245-248.

Kureishi, Y., Kobayashi, S., Amano, M., Kimura, K., Kanaide, H., Nakano, T., Kaibuchi, K. and Ito, M. (1997). Rho-associated kinase directly induces smooth muscle contraction through myosin light chain phosphorylation. *J. Biol. Chem.* **272**, 12257-12260.

Laure-Kamionowska, M., Maslinska, D. and Raczkowska, B. (2002). Discrete glioneuronal malformative lesions in the foetal and infantile cerebral cortex. *Folia Neuropathol.* **40**, 183-191.

Leung, T., Chen, X. Q., Manser, E. and Lim, L. (1996). The p160 RhoA-binding kinase ROK alpha is a member of a kinase family and is involved in the reorganization of the cytoskeleton. *Mol. Cell. Biol.* **16**, 5313-5327.

Lizard, G., Deckert, V., Dubrez, L., Moisant, M., Gambert, P. and Lagrost, L. (1996). Induction of apoptosis in endothelial cells treated with cholesterol oxides. *Am. J. Pathol.* **148**, 1625-1638.

Mauch, D. H., Nagler, K., Schumacher, S., Goritz, C., Muller, E. C., Otto, A. and Pfrieger, F. W. (2001). CNS synaptogenesis promoted by glia-derived cholesterol. *Science* **294**, 1354-1357.

Michel, J. B. (2003). Anoikis in the cardiovascular system: known and unknown extracellular mediators. *Arterioscler. Thromb. Vasc. Biol.* **23**, 2146-2154.

Micoud, F., Mandrand, B. and Malcus-Vocanson, C. (2001). Comparison of several techniques for the detection of apoptotic astrocytes in vitro. *Cell Prolif.* **34**, 99-113.

Mills, J. C., Stone, N. L., Erhardt, J. and Pittman, R. N. (1998). Apoptotic membrane blebbing is regulated by myosin light chain phosphorylation. *J. Cell Biol.* **140**, 627-636.

Mills, J. C., Stone, N. L. and Pittman, R. N. (1999). Extranuclear apoptosis. The role of the cytoplasm in the execution phase. *J. Cell Biol.* **146**, 703-708.

Nakano, K., Takaishi, K., Kodama, A., Mammoto, A., Shiozaki, H., Monden, M. and Takai, Y. (1999). Distinct actions and cooperative roles of ROCK and mDia in Rho small G protein-induced reorganization of the actin cytoskeleton in Madin-Darby canine kidney cells. *Mol. Biol. Cell* **10**, 2481-2491.

Nedergaard, M., Ransom, B. and Goldman, S. A. (2003). New roles for astrocytes: redefining the functional architecture of the brain. *Trends Neurosci.* **26**, 523-530.

Newman, E. A. (2003). New roles for astrocytes: regulation of synaptic transmission. *Trends Neurosci.* **26**, 536-542.

Pascual, M., Valles, S. L., Renau-Piqueras, J. and Guerri, C. (2003). Ceramide pathways modulate ethanol-induced cell death in astrocytes. *J. Neurochem.* **87**, 1535-1545.

Ren, X. D. and Schwartz, M. A. (2000). Determination of GTP loading on Rho. *Methods Enzymol.* **325**, 264-272.

Ren, X. D., Kiosses, W. B. and Schwartz, M. A. (1999). Regulation of the small GTP-binding protein Rho by cell adhesion and the cytoskeleton. *EMBO J.* **18**, 578-585.

Renau-Piqueras, J., Zaragoza, R., De Paz, P., Baguena-Cervellera, R., Megias, L. and Guerri, C. (1989). Effects of prolonged ethanol exposure on the glial fibrillary acidic protein-containing intermediate filaments of astrocytes in primary culture: a quantitative immunofluorescence and immunogold electron microscopic study. *J. Histochem. Cytochem.* **37**, 229-240.

Ridley, A. J. and Hall, A. (1992). The small GTP-binding protein rho regulates the assembly of focal adhesions and actin stress fibers in response to growth factors. *Cell* **70**, 389-399.

Sanai, N., Tramontin, A. D., Quinones-Hinojosa, A., Barbaro, N. M., Gupta, N., Kunwar, S., Lawton, M. T., McDermott, M. W., Parsa, A. T., Manuel-Garcia Verdugo, J. et al. (2004). Unique astrocyte ribbon in adult human brain contains neural stem cells but lacks chain migration. *Nature* **427**, 740-744.

Sebbagh, M., Renvoize, C., Hamelin, J., Riche, N., Bertoglio, J. and Breard, J. (2001). Caspase-3-mediated cleavage of ROCK I induces MLC phosphorylation and apoptotic membrane blebbing. *Nat. Cell Biol.* **3**, 346-352.

Suarez-Huerta, N., Mosselmans, R., Dumont, J. E. and Robaye, B. (2000). Actin depolymerization and polymerization are required during apoptosis in endothelial cells. *J. Cell Physiol.* **184**, 239-245.

Torgerson, R. R. and McNiven, M. A. (1998). The actin-myosin cytoskeleton mediates reversible agonist-induced membrane blebbing. *J. Cell Sci.* **111**, 2911-2922.

Ullian, E. M., Sapperstein, S. K., Christopherson, K. S. and Barres, B. A. (2001). Control of synapse number by glia. *Science* **291**, 657-661.

Valles, S., Pitarch, J., Renau-Piqueras, J. and Guerri, C. (1997). Ethanol exposure affects glial fibrillary acidic protein gene expression and transcription during rat brain development. *J. Neurochem.* **69**, 2484-2493.

van de Water, B., Nagelkerke, J. F. and Stevens, J. L. (1999). Dephosphorylation of focal adhesion kinase (FAK) and loss of focal contacts precede caspase-mediated cleavage of FAK during apoptosis in renal epithelial cells. *J. Biol. Chem.* **274**, 13328-13337.

Vermes, I., Haanen, C., Steffens-Nakken, H. and Reutelingsperger, C. (1995). A novel assay for apoptosis. Flow cytometric detection of phosphatidylserine expression on early apoptotic cells using fluorescein labelled Annexin V. *J. Immunol. Methods* **184**, 39-51.